

## ELECTRONIC STRUCTURE OF EPITAXIAL $\alpha$ -Sn<sub>1-x</sub>Ge<sub>x</sub> ALLOYS

Hartmut Höchst<sup>1</sup>, Michael A. Engelhardt<sup>1</sup> and Isaac Hernández-Calderón<sup>2</sup>

<sup>1</sup>Synchrotron Radiation Center, University of Wisconsin-Madison

Stoughton, WI 53589-3097, USA

<sup>2</sup>Depart. de Física, Centro de Investigación y Estudios Avanzados del Instituto Politécnico  
Nacional, CINVESTAV, Mexico D. C.

### SUMMARY

The electronic structure and interface properties of  $\alpha$ -Sn<sub>1-x</sub>Ge<sub>x</sub> alloy films grown by molecular beam epitaxy (MBE) on GaSb, CdTe and Ge(100) were studied by angle resolved synchrotron radiation photoemission spectroscopy (ARPES). Deposition at temperatures below ~150 C results in polycrystalline or amorphous films. At higher substrate temperatures GaSb and CdTe partially react with the overlayer forming either GeSb or SnTe in the interface region. Homogeneous alloy films with good crystalline quality were grown on Ge(100) at ~400 C up to a critical thickness of 200-300 Å. Photoemission core level analysis indicates a strong tendency to form an ordered compound with a composition close to x~0.5. Angle resolved valence band spectra show the shift of the  $\Gamma_8$  point from ~0.6 eV in Ge(100) to ~0.16 eV below  $E_F$  in the  $\alpha$ -Sn<sub>0.48</sub>Ge<sub>0.52</sub> alloy. The experimental information of a constant alloy Fermi level locates the top of the  $\Gamma_8$  valence band ~0.16 eV below  $E_F$ . Assuming a linear band model, the direct band gap of  $E_g$ ~0.2 eV for x~0.5 will then locate the bottom of the  $\Gamma_7$  conduction band ~0.04 eV above  $E_F$ .

### 1. INTRODUCTION

$\alpha$ -Sn is a diamond structured, symmetry induced, zero gap semiconductor with very interesting electronic properties. In order to utilize  $\alpha$ -Sn based material in semiconducting devices such as IR-detectors one should be able to open and tailor the band gap. Band gap engineering should be possible by alloying  $\alpha$ -Sn with Ge [1]. Assuming a linear relationship between the band structure of both components, the negative  $\Gamma_7$ - $\Gamma_8$  band gap would be zero and would reverse the order at Ge concentrations of x~0.35. Further addition of Ge should open the direct band gap up to 0.55 eV for x~0.78. However, the growth of  $\alpha$ -Sn and  $\alpha$ -Sn<sub>1-x</sub>Ge<sub>x</sub> alloys is not straightforward and is particularly challenging since the  $\alpha$ -phase is metastable and Ge is nearly immiscible in bulk Sn.

The  $\alpha$ -phase of bulk Sn is only stable below 13.2 C [2] while thin films grown heteroepitaxially on CdTe and InSb are substrate stabilized with  $\alpha$ - $\beta$  transition temperatures ranging well above 100 C [3-7]. Low temperature transport measurements of high quality MBE grown  $\alpha$ -Sn and  $\alpha$ -Sn<sub>1-x</sub>Ge<sub>x</sub> alloys indicate n-type behavior with  $n_d$ ~3·10<sup>17</sup> cm<sup>-3</sup> and mobilities of several times 10<sup>4</sup> cm<sup>2</sup>/Vsec [8,9]. Besides the problem of the  $\alpha$ - $\beta$  phase stability, one should also consider interfacial strain caused by the lattice mismatch between the substrate and the alloy film. Strain can be an additional disadvantage and may contribute to the

instability of the thermodynamic metastable  $\alpha$ -phase of  $\text{Sn}_{1-x}\text{Ge}_x$  alloys. Conventional growth techniques which work under thermodynamic equilibrium are thus not suitable for the fabrication of the metastable  $\alpha\text{-Sn}_{1-x}\text{Ge}_x$  alloys.

Single crystalline and amorphous, tetrahedrally coordinated alloys, with compositions reaching  $x \sim 0.5$  were grown by modified sputter deposition techniques [10-13]. Alloy mixing on an atomic scale was indicated by small angle X-ray scattering experiments [12,13]. Utilizing non-equilibrium growth techniques it appears to be possible to grow metastable  $\alpha\text{-Sn}_{1-x}\text{Ge}_x$  alloys.

We report on *in situ* photoemission experiments to investigate the structural and electronic properties of MBE grown  $\alpha\text{-Sn}_{1-x}\text{Ge}_x$  films. Photoemission spectroscopy (ARPES) has been used to determine the electronic valence band structure of the  $\alpha\text{-Sn}_{1-x}\text{Ge}_x$  alloys.

## 2. EXPERIMENTAL

Thin  $\alpha\text{-Sn}_{1-x}\text{Ge}_x$  films were grown by MBE on CdTe, GaSb and Ge(100) substrates. The substrates were cleaned with organic solvents and rinsed with deionized water before they were loaded into the MBE system. Prior to the MBE growth the surfaces were cleaned by *in situ* sputtering for several hours with Ar ions at an energy of 500 eV. To remove the sputter damage, CdTe had to be annealed for 5-10 min. at  $\sim 270$  C. GaSb was annealed to 320 C, while Ge required annealing up to  $\sim 600$  C. The improved surface order was monitored during the anneal by reflection high energy electron diffraction (RHEED). The removal of surface contaminations was followed by soft X-ray core and valence band photoemission spectroscopy.

Tin and germanium were evaporated out of boron nitride crucibles from liquid nitrogen shrouded effusion cells. The evaporation rates, which were typically several Å/min, were measured with calibrated and temperature stabilized quartz crystal monitors. Photoemission experiments performed *in situ* on the substrates and on the epilayers utilized the synchrotron radiation of the University of Wisconsin's electron storage ring ALADDIN. Photoelectrons were collected at normal emission along the [001] axis of the crystal plates while the synchrotron radiation was directed along the [110] direction with an angle of incidence of 60° with respect to the sample normal. The total energy resolution resulting from the combined finite band pass of the monochromator and electron spectrometer ranged from  $\Delta E \sim 0.18$  eV at the lower photon energies to  $\Delta E \sim 0.35$  eV at  $h\nu \sim 100$  eV.

## III. RESULTS AND DISCUSSION

A major concern for any epitaxial growth is the choice of a proper substrate. Besides the necessary prerequisite of having the desired crystal structure and lattice match with the overlayer film, it is also important that the substrate is non-reactive with the epilayer. The constraints for lattice matching an alloy film with a particular substrate can always be achieved by using ternary compound semiconductors; however, the requirement of a non reactive substrate is usually harder to fulfill.

We investigated GaSb, CdTe and Ge(100) for growth studies of the  $\alpha\text{-Sn}_{1-x}\text{Ge}_x$  alloys.

Assuming a linear relation of the alloy lattice constants GaSb would be lattice matched with an alloy of  $x \sim 0.5$ . Depositing films of the same concentration on Ge(100), which has a  $\sim 6\%$  smaller lattice constant, results in compressive strain while films grown on CdTe are under tensile stress of roughly the same magnitude.

Surface sensitive photoemission spectra of the substrate core level attenuation, as well as Sn and Ge core spectra from the interfaces and overlayers grown under various conditions on GaSb(100) indicate surface segregation and increased interfacial reactivity. Fig. 1 shows the normalized Sn4d/Ge3d photoemission intensity of alloy films with nominal composition  $x \sim 0.5$  which were deposited at various substrate temperatures. Growth at  $T_{\text{sub.}} = 25\text{ C}$  increases the relative Sn concentration near the surface by a factor of  $\sim 2$  for a  $60\text{\AA}$  thick film. Higher growth temperatures reduce the Sn segregation considerably. At  $T_{\text{sub.}} = 250\text{ C}$  the Sn/Ge ratio is only  $\sim 1.3$  for a film of the same thickness. However, deposition at  $T_{\text{sub.}} = 450\text{ C}$  alters the composition and shows relative Ge enrichment.

The attenuation of the substrate Sb4d and Ga3d emission is also drastically affected by the growth temperature. With increasing substrate temperatures we found Sb to be less attenuated than Ga. Since we do not see any significant shift nor the appearance of an additional Sb feature, we are inclined to rule out the possibility that metallic Sb diffuses towards the surface. Even though we do not see any chemically shifted components, it is most likely that the surface region contains reacted GeSb at elevated growth temperatures.

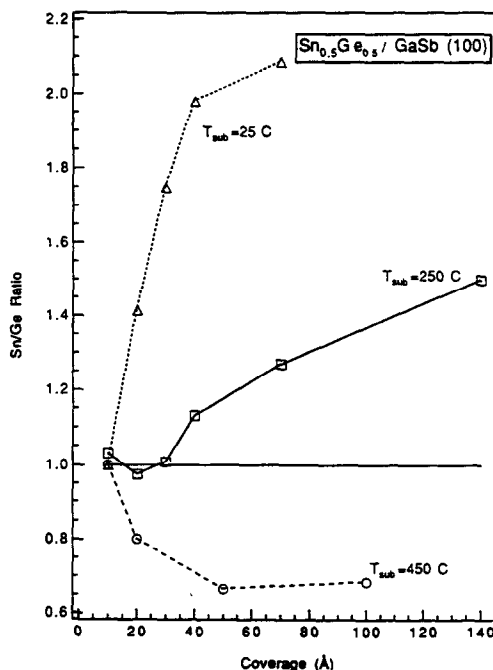


Fig. 1: Photoemission intensity ratio between Sn4d and Ge 3d spectra of  $\text{Sn}_{0.5}\text{Ge}_{0.5}$  films grown at different temperatures on GaSb(100).

Growth on CdTe(100) substrates shows basically the same trend [14]. At lower substrate temperatures, surface mobilities of the adsorbed atoms are too small to allow the formation of a smooth overlayer. Increasing the substrate temperature improves the structural quality of the overlayer, but also increases the interfacial reactivity. At  $T_{\text{sub.}} \sim 160\text{-}200\text{ C}$  Sn4d core spectra which are shown in Fig.2, clearly indicate the appearance of a second chemically shifted component. The reacted product is most likely SrTe [15].

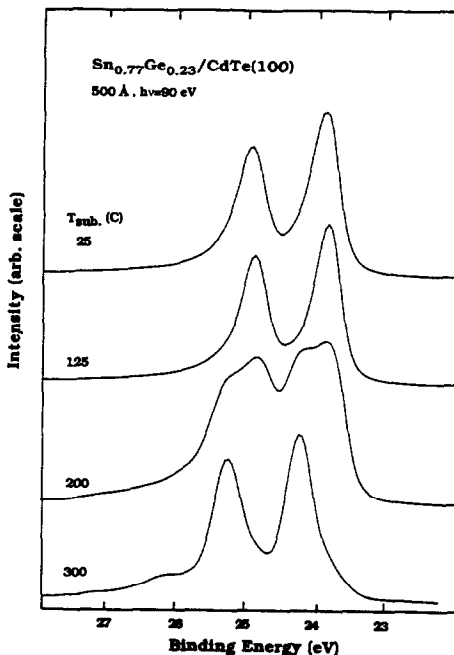


Fig.2 : Sn4d core spectra of 500 Å  $\text{Sn}_{0.77}\text{Ge}_{0.23}$  grown at different temperatures on CdTe(100)

Due to the insolubility of Sn in Ge, interfacial compound formation is not possible with Ge substrates. However, the overlayer will be forced to grow under considerable compressive strain which may destabilize the single crystal growth. The presence of  $\sim 6.5\%$  lattice mismatch allows only the first few layer to grow with a smooth, atomically flat, surface. After the deposition of  $10\text{-}20\text{\AA}$  the streaked RHEED pattern turns into the spotted three dimensional bulk pattern of an ordered overlayer. Films  $300\text{\AA}$  thick still gave fairly sharp and dispersive transition features in the angle resolved photoemission spectra. We consider this as additional indirect evidence for crystalline order when ARPES is used to determine the bulk electronic properties.

With increasing deposition temperatures the valence band spectrum changes from a broad unstructured feature into a three peak spectrum. Growth at  $200\text{ C}$  clearly shows the onset of sharper structures which develop further at higher growth temperatures. However, it is

interesting to note that even at low growth temperatures there is no indication of precipitation of the metallic  $\beta$ -Sn phase. The alloy spectra do not show the Fermi-level emission which is typical for a  $\beta$ -Sn film [14,16].

Higher substrate temperatures increase the surface mobility and allow a much smoother film growth. Above 200 C the spotty RHEED pattern is basically free of the ring structures typical of polycrystalline growth. With higher substrate temperatures sharper direct transition structures appear in the angle resolved photoemission spectra. Since direct ( $k$  conserving) transitions strongly depend on the absence of surface scattering, their relative intensity increase can be used as indirect evidence of the improved crystalline order.

Figure 3 shows normal emission valence band spectra measured at different photon energies. With increasing photon energies the emission features at the top of the valence band show a considerable dispersion. A comparison with the spectra of Ge(100) clearly shows the additional alloy emission in the gap region. The top of the alloy valence band shows a significant shift at  $h\nu=16$  eV towards  $E_F$ . At  $h\nu\sim 20$  eV a shoulder appears  $\sim 0.16$  eV below  $E_F$ . Emission from the 2. valence band starts at  $\sim 1.5$  eV for  $h\nu=16$  eV and disperses to  $\sim 6.2$  eV for  $h\nu=28$  eV. We did not attempt to perform a detailed band mapping of the valence bands but it should be noted that the alloy spectra closely follow the experimentally determined as well as the calculated dispersion of the Ge valence bands along the  $\Gamma$ -X direction [17,18].

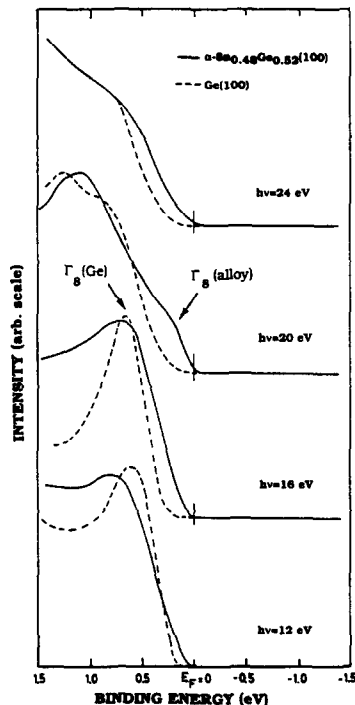


Fig. 3: Comparison of photoemission spectra around the top of the valence band of a 300 Å thick  $\alpha$ - $\text{Sn}_{0.48}\text{Ge}_{0.52}(100)$  film with spectra of Ge(100) measured at different photon energies.

The dispersion of the lower lying valence bands of the  $\alpha\text{-Sn}_{1-x}\text{Ge}_x$  alloy follows that of Ge for larger  $k$  values along  $\Gamma\text{X}$ . Closer to the top of the valence bands both materials show pronounced differences. Since the closest feature to the Fermi level is observed for the alloy at  $E_B\sim0.16$  eV and the Ge 3d core level did not show any shifts which could be related to band bending effects, we can safely assume that the emission at  $\sim0.16$  eV is due to transitions from the top of the alloy valence band. The observed peak is thus an indication of the expected narrowing of the alloy band gap. Assuming a linear behavior between the  $\Gamma_8$  valence band and the  $\Gamma_7$  conduction band, the direct energy gap for an alloy with  $x=0.48$  would be  $\sim0.2$  eV. Using the additional experimental information of a constant Fermi level, we can then assign the position of conduction band minimum to be  $\sim0.04$  eV above  $E_F$ .

One may speculate that the addition of Ge may help to raise the phase transition temperature even further [2,3]. Assuming a simple linear relationship between the  $\alpha\text{-}\beta$  transition temperatures for  $T_{\text{Sn}}=13.2$  C and  $T_{\text{Ge}}=932.5$  C, the phase transition temperature would increase by about  $\sim9$  C/% Ge. However, due to the metastable nature of the alloy it may be more appropriate to expect alloy parameters to show a considerable bowing effect.

Magneto transport measurements on  $\alpha\text{-Sn}_{1-x}\text{Ge}_x$  alloys showed a strain induced shift of the  $L_6$  conduction band. [8]. Presently we do not have experimental evidence of strain induced shifts in the alloy valence bands. Photoemission spectroscopy is probably not sensitive enough to detect the effect of lattice strain other than some additional line-shape broadening. Since films of the thickness up to 300Å still show a large degree of order and relatively sharp transitions, they were used to study the bulk electronic structure by ARPES.

The data shown in Fig.3 were obtained from a flux ratio of  $n_{\text{Sn}}/n_{\text{Ge}}=3$ . Assuming a unit sticking coefficient for both source materials the offered flux ratio should deposit a film containing 25% Ge. Based on Sn4d and Ge3d photoemission intensities of the deposited alloys (which were normalized to the intensity of pure  $\alpha\text{-Sn}$  and Ge(100) surfaces) we determined the composition of the deposited material with an estimated accuracy of  $\pm5\%$ . Our core level analysis indicates a strong compositional deviation in the deposited films compared to that of the molecular beams.

One may argue that the differences between the photoemission spectra of the alloy and those of Ge(100) are caused by the precipitation of Sn droplets floating on top of the Ge substrate rather than by an alloy formation. The possibility of that happening is certainly large, keeping in mind that the alloy is a thermodynamically unstable bulk system where both components are nearly insoluble in each other. However, the absence of a Fermi level emission and Sn4d core level spectra showing a small energy shift compared to the metallic  $\beta\text{-Sn}$  phase led us assume that Sn and Ge are homogeneously mixed in our thin alloy films [19].

A test to demonstrate the absence of larger Sn clusters in the  $\alpha\text{-Sn}_{1-x}\text{Ge}_x$  alloy films is given in Fig.4 where we show the photoemission cut off spectrum in comparison with those of  $\alpha\text{-Sn}(100)$  and Ge(100). The position of the photoemission cut off depends on the work function of the material and can be easily distinguished from that of the electron analyzer by biasing the sample with a small voltage. The spectra in Fig.4 are plotted versus the work function  $\phi$  which

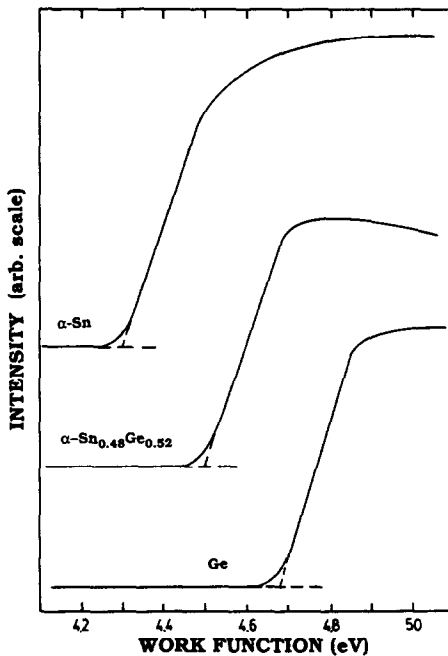


Fig. 4: Comparison of the work function of a 200 Å thick  $\alpha\text{-Sn}_{0.48}\text{Ge}_{0.52}$  film grown at 400 C on Ge(100) with that of elemental  $\alpha\text{-Sn}$ (100) and Ge(100) surfaces.

can be determined by  $\phi = hv - E_F$ . As can be seen from Fig.4, the alloy work function agrees well with a linear model extrapolating between the work function of both alloy components. In case of larger metallic Sn clusters on top of the Ge(100) surface, the alloy spectrum should show a stepped cut off consisting of a superposition of the Ge and  $\beta\text{-Sn}$  spectra. The work function of  $\beta\text{-Sn}$  is  $\sim 0.1$  eV smaller than that of the  $\alpha$ -phase [16] and should thus be easy to detect as a step in the cut off spectrum at  $\phi \sim 4.2$  eV.

The question of whether the additional Sn atoms which are not incorporated in the alloy lattice diffuse into the Ge substrate or reevaporate from the surface cannot be answered from our present experiments. It should be noted that DiCenzo et al. [20] deposited Sn on Ge(111) at room temperature and found that annealing a submonolayer to 550 C changed the surface coverage by not more than 5%. Annealing of a higher coverage, however, resulted in a stronger decrease of Sn and was attributed to reevaporation.

Diffusion may also contribute to some extent to balance the missing masses but it should be kept in mind that the fairly large coefficients of the substitutional diffusion of Sn into Ge ( $\sim 10^{-12} \text{ cm}^2/\text{s}$  at 500 C) are most likely misleading for the present study [21]. Since the determination of diffusion coefficients assumes Fick's law to describe the diffusion process it may not be appropriate to use it for a system which is insoluble.

Our core level analysis could rather be interpreted as a strong tendency to form a compound with

a composition close to  $x \sim 0.5$ . The results from Shevchik and Paul [13], who found a surprising compositional homogeneity in their sputtered SnGe compound films, already indicate the preference to form bonds with next nearest neighbors of the opposite kind. The MBE growth of a zinc-blende type  $\alpha$ -SnGe compound may thus be thermodynamically more favorable than the growth of a statistically distributed substitutional diamond structured alloy.

The observed composition pinning is not unusual and has been seen for the coherent epitaxial growth of other alloys [22]. Alloy films of materials where the bulk constituents are immiscible were recently grown as stoichiometric compounds by MBE. Total energy calculations [23] using thermodynamic functions of the free energies and formation enthalpies for bulk and epitaxial growth were able to predict the observed stability of ordered epitaxial phases at growth temperatures well below the miscibility-gap temperature. The thermodynamic model calculations indicates that it is energetically more favorable for thin alloy films to minimize energy by lattice matching within the alloy rather than between the alloy and the substrate [24].

#### 4. CONCLUSIONS

Growth studies utilizing CdTe as well as lattice matched GaSb substrates indicate increased interfacial reactivity at the desired growth temperatures. At substrate temperatures of  $\sim 160$ - $200$  C CdTe starts to react with Sn forming a SnTe compound at the interface region while at temperatures above  $\sim 250$  C GaSb interacts with the overlayer. The reaction product in this case is most likely GeSb.

Alloys of  $\alpha$ - $\text{Sn}_{1-x}\text{Ge}_x$  can be grown as thin films by MBE on Ge(100) substrates. Angle resolved valence band photoemission spectra and RHEED indicate good crystalline order for alloys grown at substrate temperatures  $T_{\text{sub.}} \sim 400$  C.

Core level intensity measurements indicate a preferred growth of the alloy with  $x \sim 0.5$ . The thermodynamic driving force for the growth of an ordered metastable compound seems to be fairly large. Compositional pinning in the epitaxial alloy was observed over a wide range of flux ratios.

Work function measurements indicate the growth of a homogeneous alloy without the precipitation of metallic tin clusters.

Angle resolved photoemission spectroscopy provides evidence of the expected band gap closing by alloying Sn with Ge. For thin alloy films with  $x \sim 0.52$  we found a shift of the valence band maximum  $\Gamma_g$  to  $\sim 0.16$  eV below  $E_F$ . Considering the experimental fact that  $E_F$  does not significantly shift from its position in Ge(100), we predict  $\Gamma_g$  to be  $\sim 0.16$  eV below  $E_F$ . According to the linear band model the direct gap for an alloy with  $x \sim 0.52$  would be  $E_g \sim 0.2$  eV which places the bottom of the conduction band  $\Gamma_7$   $\sim 0.04$  eV above the Fermi level.

#### ACKNOWLEDGEMENTS

Research funded by SDIO-IST and managed by NRL under contract No: N00014-86-K-2022. The Synchrotron Radiation Center is funded through an NSF operations grant.

## REFERENCES

1. S. Oguz, W. Paul, T.F. Deutsch, B-Y. Tsaur, and D.V. Murphy, *Appl. Phys. Lett.* **43**, 848 (1983).
2. G. A. Busch and A. Kern, *Solid State Physics*, edited by H. Ehrenreich, F. Seitz, and D. Turnbull (Academic Press, New York, 1961), Vol. 11.
3. R. F. C. Farrow, D. S. Robertson, G. M. Williams, A. G. Cullis, G. R. Jones, I. M. Young, and P. N. J. Dennis, *Cryst. Growth* **54**, 507 (1981).
4. H. Höchst, and I. Hernández-Calderón, *Surf. Sci.* **126**, 25 (1983).
5. J. Menendez, and H. Höchst, *Thin Solid Films*, **111**, 375 (1984).
6. L. Vina, H. Höchst, and M. Cardona, *Phys. Rev. B* **31**, 958 (1985).
7. I. Hernández-Calderón, and H. Höchst, *Phys. Rev. B* **25**, 4961 (1983).
8. C. A. Hoffman, J. R. Meyer, R. J. Wagner, F. J. Bartoli, M. A. Engelhardt, and H. Höchst, to be publ. *Phys. Rev. B*
9. L.-W. Tu, G. K. Wong, and J.B. Ketterson, *Appl. Phys. Lett.* **54**, 1010 (1989) A. W. Ewald, J. *Appl. Phys.* **25**, 1436 (1954).
10. T. Soma, H. Matsuo, and S. Kagaya, *phys. stat. sol. (b)* **105**, 311 (1981).
11. J. B. Bean, *J. Vac. Sci. Technol.* **B4**, 1427 (1986).
12. S. L. Shah, J. E. Greene, L. L. Abels, Q. Yao, and P. N. Raccah, *Journal of Crystal Growth* **83**, 3 (1987).
13. N. J. Shevchik, and W. Paul, *J. of Non-Crystalline Solids* **16**, 55 (1974).
14. I. Chambouleyron, F. C. Marques, J. P. de Souza, and I. J. R. Baumvol, *J. Appl. Phys.* **65**, 1591 (1989).
15. H. Höchst, D. W. Niles, M. A. Engelhardt, and I. Hernández-Calderón, *J. Vac. Sci. Technol. A* **7**, 775 (1989).
16. H. Höchst and I. Hernández-Calderón, *J. Vac. Sci. Technol. A* **3**, (1985).
17. T. C. Hsieh, T. Miller, and T.-C. Chiang, *Phys. Rev. B* **30**, 7005 (1984).
18. J. R. Chelikowsky, and M. L. Cohen, *Phys. Rev. B* **14**, 556 (1976).
19. H. Höchst, M.A. Engelhardt, and I. Hernández-Calderón, to be publ.
20. S. B. DiCenzo, P. A. Bennett, D. Tribula, P. Thiry, G. K. Wertheim, and J. E. Row, *Phys. Rev. B* **32**, 2330 (1985).
21. *Landoldt-Börnstein*, Neue Serie Band 17, Herausgeber: O. Madelund, M. Schulz, H. Weiss, (Springer-Verlag Berlin, Heidelberg, New York, Tokyo 1984) p. 118 ff.
22. M. J. Jou, Y. T. Cherng, H. R. Jen, and G. B. Stringfellow, *Appl. Phys. Lett.* **52**, 549 (1988).
23. D. M. Wood, and A. Zunger, *Phys. Rev. Lett.* **61**, 1501 (1988).
24. D. M. Wood, and A. Zunger, *Phys. Rev. B* **36**, 7994 (1987)